Soft-Probe-Scanning Electrochemical Microscopy reveals electrochemical surface reactivity of *E. coli* biofilms

- Supplementary Information -

Sorour Darvishi,[a] Horst Pick,[b] Emad Oveisi,[c] Hubert H. Girault,*[a] and Andreas Lesch*[d]

[a] Ecole Polytechnique Fédérale de Lausanne (EPFL) Valais Wallis, Laboratory of Physical and Analytical Electrochemistry, Rue de l'Industrie 17, 1950 Sion, Switzerland.

[b] Environmental Engineering Institute, GR-LUD, Ecole Polytechnique Fédérale de Lausanne (EPFL), School of Architecture, Civil and Environmental Engineering, EPFL Station 2, 1015 Lausanne, Switzerland.

[c] Interdisciplinary Center for Electron Microscopy, École Polytechnique Fédérale de Lausanne (EPFL), CH-1015 Lausanne, Switzerland.

[d] University of Bologna, Department of Industrial Chemistry "Toso Montanari", Viale del Risorgimento 4, 40136 Bologna, Italy.

* CORRESPONDING AUTHOR FOOTNOTE

EMAIL: andreas.lesch@unibo.it TEL: +39 051 2093701

EMAIL: hubert.girault@epfl.ch TEL: +41 21 6933151

List of supplementary information:

SI-1. Confocal laser scanning fluorescence microscopy imaging

Staining with CTC/DAPI:

CTC and DAPI offer a fast, facile, and reliable method for the metabolic investigation of bacteria in both suspension and attached to surfaces [1]. CTC is a monotetrazolium redox stain that produces a red fluorescent formazan. Red formazan forms when CTC is chemically or biologically reduced [2]. DAPI observes the DNA in cells. The DAPI staining method does not penetrate living bacterial cells and shows the amount of eDNA in living biofilms [3].

For CTC staining, a solution of 50 mM CTC was prepared in PBS. 20 µL were dropped on the biofilm-coated glass coverslip and incubated for 2 h at 37 °C. The absorption wavelength and emission wavelength of CTC are 480 nm and 630 nm, respectively.

For DAPI staining, 1 µg/mL of DAPI in DMSO was prepared. 300 µL of the solution was dropped on the biofilm-coated glass coverslip and incubated for 10 min at room temperature. The absorption wavelength and emission wavelength of DAPI are 358 nm and 461 nm, respectively.

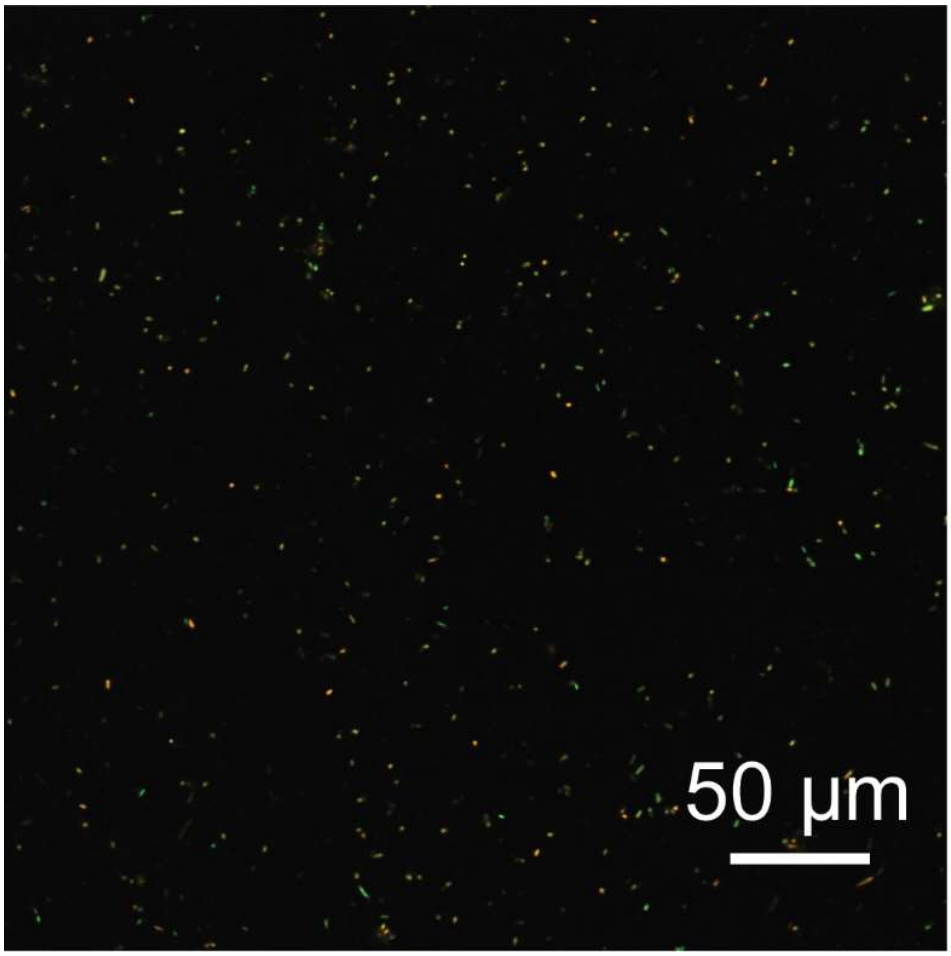

Figure S1-1. Confocal laser scanning fluorescence microscope images of three-days old *E. coli* biofilm co-stained with SYTO 9 (green) and PI (yellow).

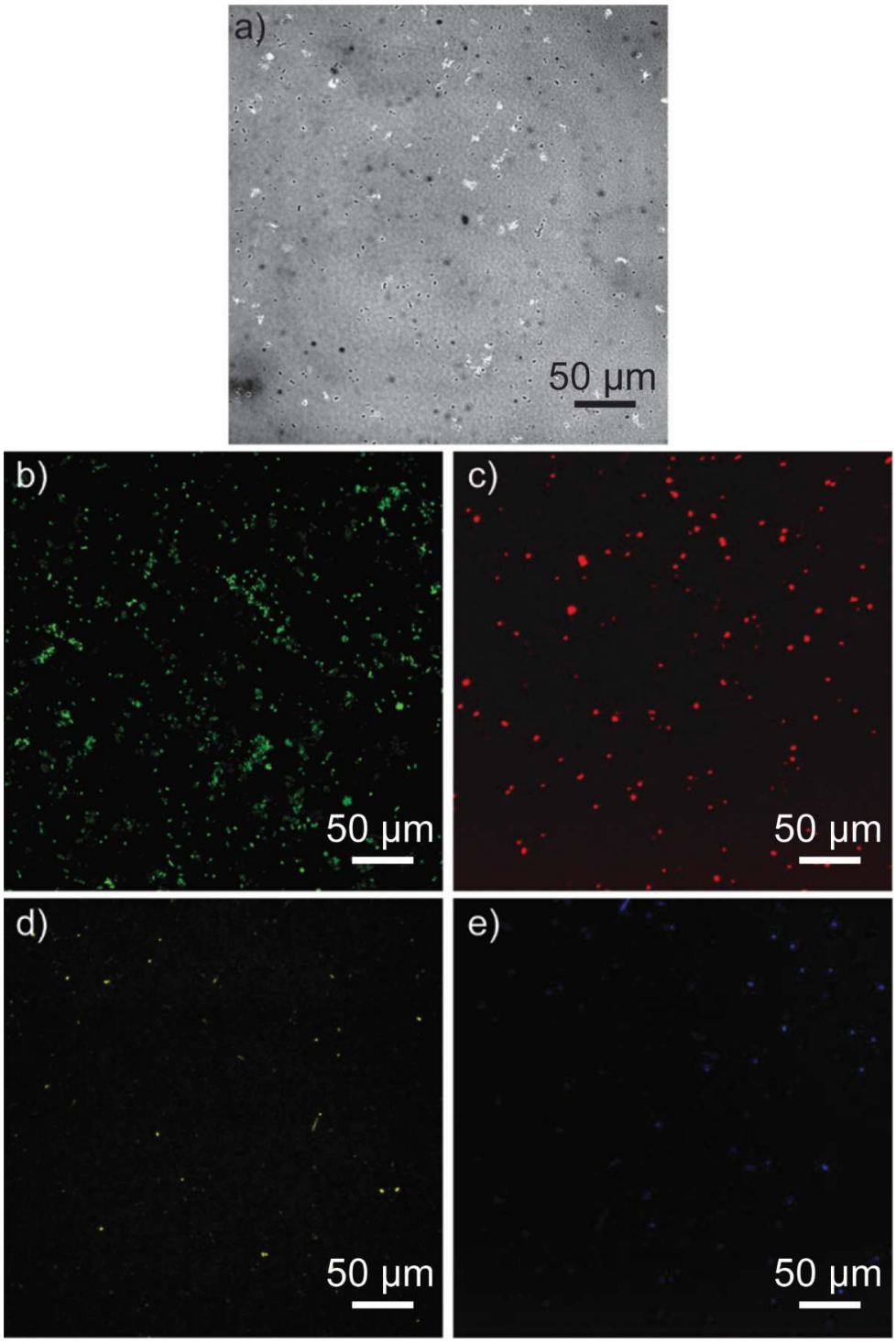

Figure S1-2. Confocal laser scanning fluorescence microscope images of one-day-old biofilm. (a) Bright field, (b) SYTO 9 staining, (c) CTC staining, (d) PI staining, and (e) DAPI staining. Confocal fluorescence images (a), (b), and (d) were in the same area of the sample. Confocal fluorescence images (c) and (e) were in the same area of the sample.

SI-2. Scanning electron microscopy (SEM) of *E. coli* biofilm

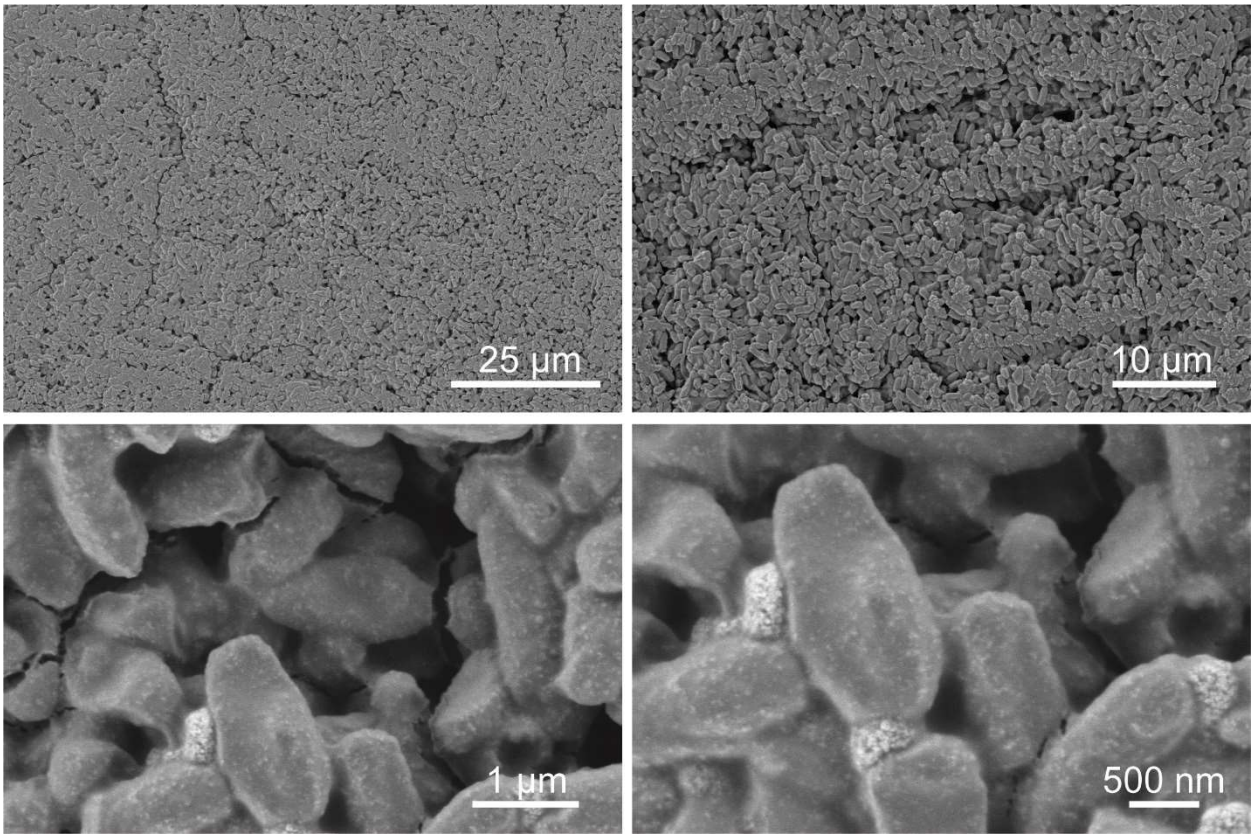

Figure S2-1. Scanning electron microscopy images of one-day-old *E. coli* biofilm with four different magnifications.

Biofilm structure

Biofilms are micro-organisms in which microbes produce extracellular polymeric substances (EPS). EPS includes proteins (<1-2%, including enzymes), DNA (<1%), polysaccharides (1-2%) and RNA (<1%). Water (up to 97%) is the major part enabling the transport of nutrients inside the biofilm matrix [4]. **Fig. S2-2** shows EPS-covered *E. coli* cells. The bacterial cell in the center is dividing, which makes the EPS layer very clear.

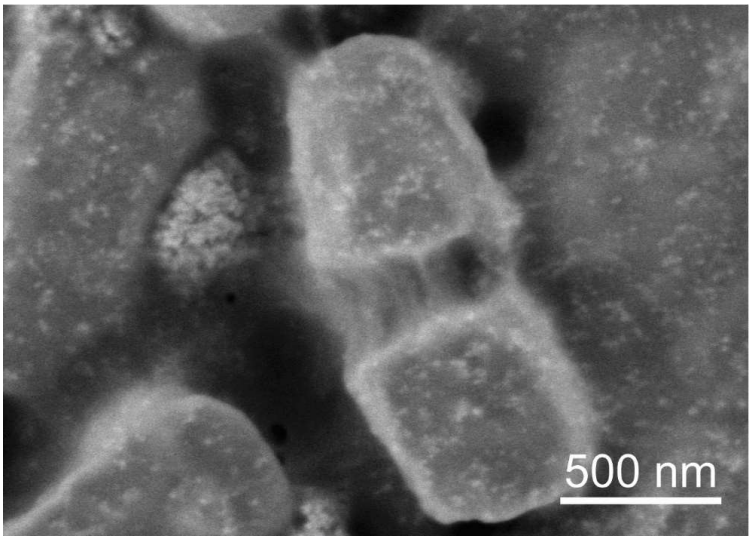

Figure S2-2. Scanning electron microscopy image of a dividing *E. coli* cell. *E. coli* cells are clearly covered by a connecting EPS layer.

Another proof for the existence of the EPS layer is shown in the SEM of **Fig. S2-3**. The EPS layer divided, maybe due to drying under ultra-high vacuum conditions or because bacterial cells started the process of detaching [5].

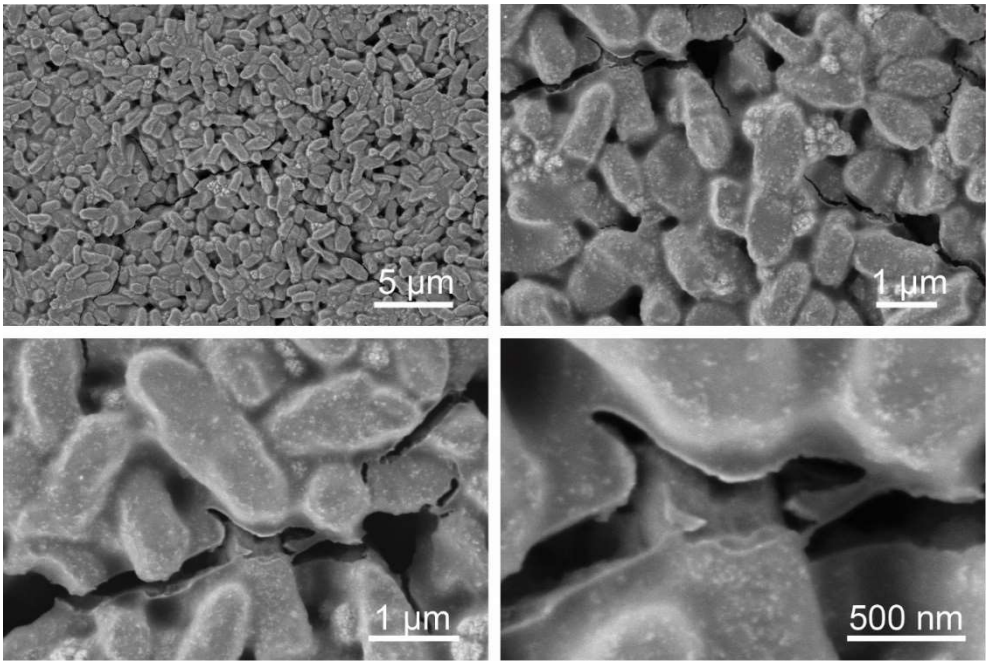

Figure S2-3. Scanning electron microscopy images of a biofilm with a cracked EPS layer demonstrating its presence.

SI-3. Soft-Probe-SECM

A soft SECM probe containing a carbon paste microelectrode was made as previously reported (Cortes-Salazar et al. 2010) [6].

During approach curves, the soft probe is tilted by an angle of 20° in respect to the surface normal. For approach curve analysis, the probe height h_P is considered instead of the working distance d (**Fig. S3-1**). h_P is positive when the soft probe is in solution, it becomes zero when the deepest part of the soft probe touches the sample ($h_P = 0$, $d > 0$) and negative when it is pressed against the substrate ($h_P < 0$, $d > 0$)

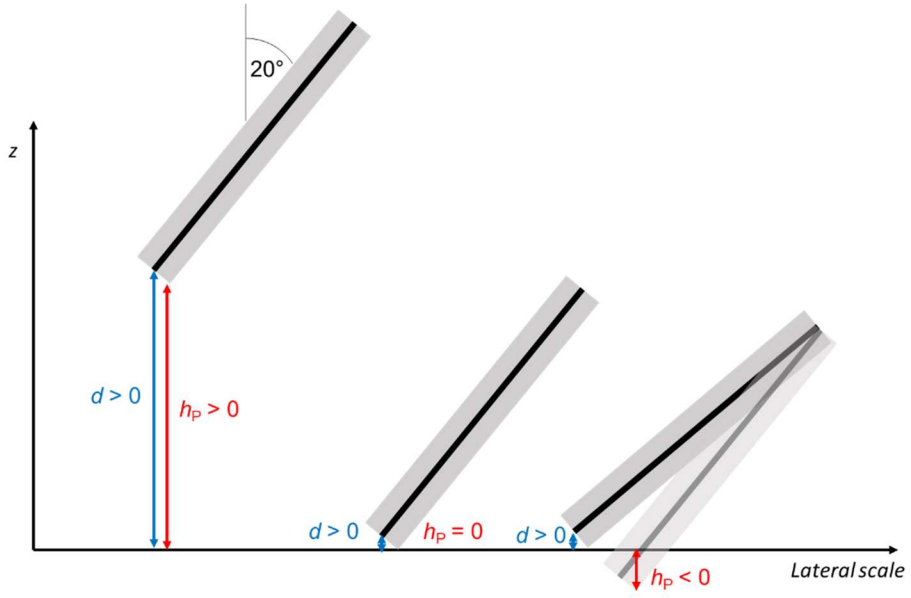

Figure S3-1. Schematic representation of the meaning of the probe height h_P and the relation to the working distance d between active part of the soft probe and the sample surface.

The SECM probe angle was controlled by the SECM probe holder. Once the probe touched the substrate surface, slight bending of the SECM probe on the plastic sets in while the SECM current remains nearly constant, demonstrating the constant working distance. The probe during that period is pressed against the substrate by moving the SECM probe holder downwards to reach an h_P = -35 µm (vertical distance of the probe after the probe had contacted the substrate surface). The h_P ranged herein generally from -25 µm to -35 µm. More information can be found in our previous works [6].

Video recordings of a soft probe approaching the substrate and performing a contact mode line scan are provided as additional material (**Movie SI-5** and **Movie SI-6**). **Fig. S3-2** shows a freeze-frame of the line scan video while the soft probe was translated over the biofilm-coated area.

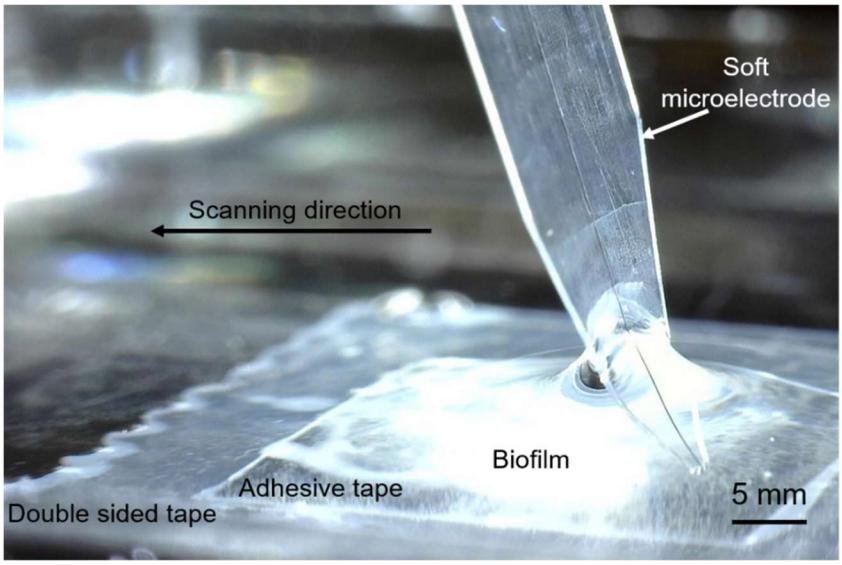

Figure S3-2. Soft-Probe-SECM over tape collected biofilm. Photo for demonstration purposes. Experiments were always carried out in an electrochemical cell with QRE and CE.

SI-4. The thickness of the biofilm on glass slide and adhesive tape

Thickness of one-day-old *E. coli* biofilm on glass:

The thickness of a one-day-old biofilm on a glass slide was determined at air by using a laser scanning micrograph, as shown in **Fig. S4-1**. The biofilm thickness was extracted from a 2D profile created in the microscope software and resulted in being up to 10 µm with a distance of 1 mm from the biofilm edge.

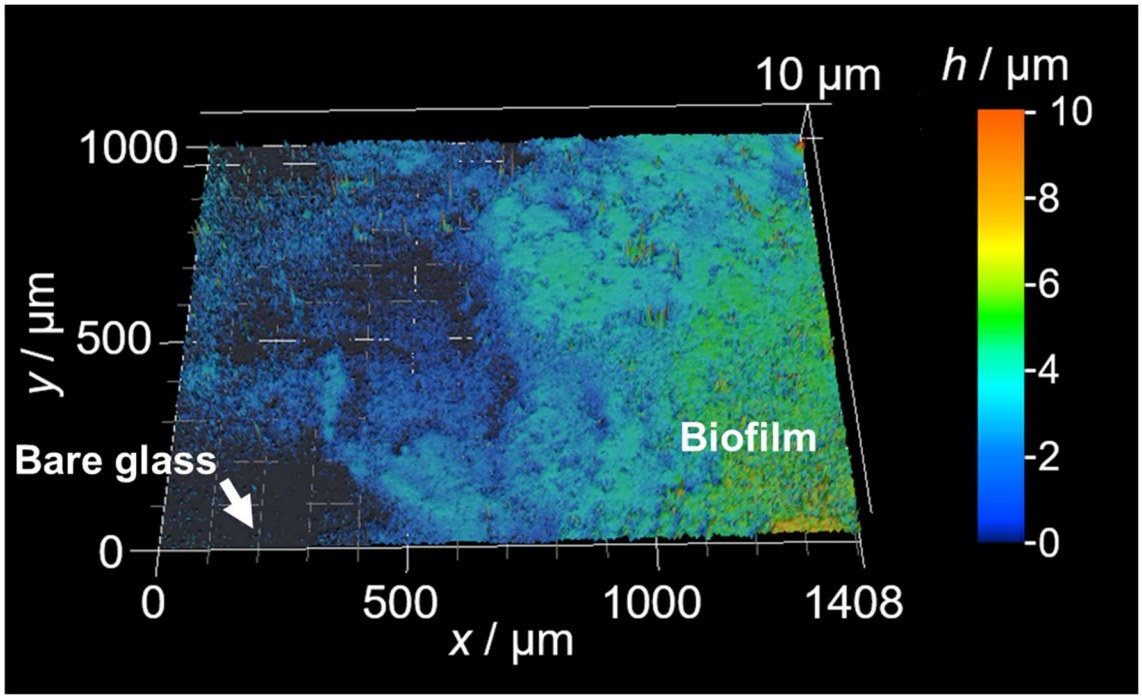

Figure S4-1. Laser scanning micrograph of one-day-old biofilm grown on the glass slide.

Thickness of tape-collected surface layer of one-day-old *E. coli* biofilm on glass:

The thickness of the top layer of a one-day-old biofilm, which was removed from the glass slide with adhesive tape, was estimated from SEM images taken from a cross-section of the adhesive tape (**Fig. S4-2a**). ImageJ (1.52a, USA) software was used for measuring the thickness of the biofilm layer from the high magnification SEM image in **Fig. S4-2b**. Most likely due to the limited resolution of the tape-stripped biofilms as a result of the exposure of large areas of plastic to the electron beam, individual bacterial cells cannot be seen. Sputtering conductive layers on this kind of sample was not possible. The thickness of the vacuum-dried biofilm on tape in ten different places (separated by 2 µm) was determined. The diameter of living individual *E. coli* cells is ~1 µm. Therefore, some of the following values indicate that several parts of the collected biofilm on

the adhesive tape were not covered by bacterial cells. The following values were measured: 1.15 µm, 1 µm, 0.06 µm (no bacterial cells), 1.43 µm, 3.35 µm, 0.213 µm (no bacterial cell), 3.17 µm, 2.98 µm, 0.54 µm (no bacterial cell), and 0.03 µm (no bacterial cell). The average and standard deviations are 2.2 µm and 1.1 µm, respectively.

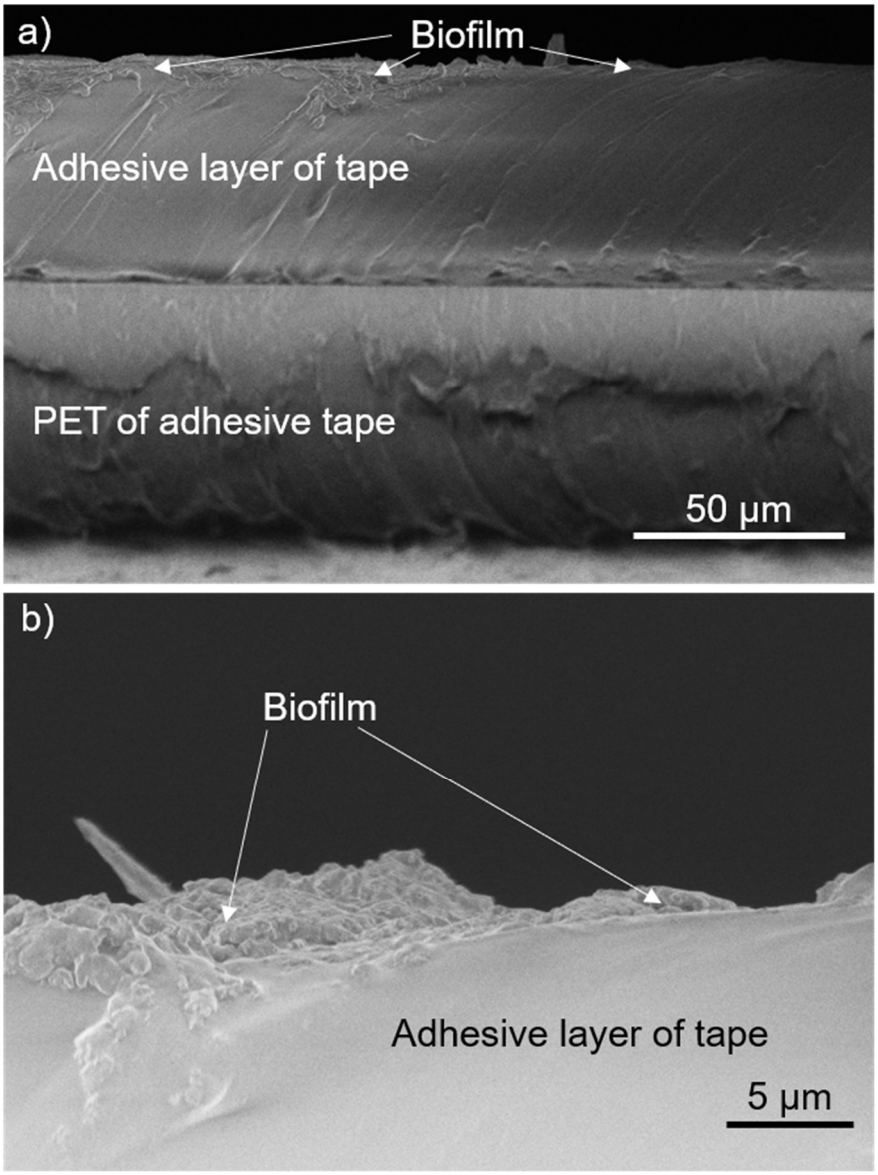

Figure S4-2. Scanning electron microscopy images of the cross-section of adhesive tape covered with the surface layer of a one-day-old biofilm taken from a biofilm on glass. (a) and (b) are imaged with two different magnifications.

SI-5. Crystal violet staining of biofilm

Crystal violet staining is the gold standard method for visualizing quantitatively *in vitro* biofilm formation [7]. However, it does not give a measure of biofilm viability. It stains both the bacterial cells and the extracellular matrix [8]. The method shows some limits, such as that some material could be washed away during sample preparation. Further, the solubility of the exopolymers is dependent on the choice of the extraction fluid. Because the quantity of exopolysaccharides (EPS) present in biofilms is low, it is often necessary to increase the total area colonized by the cells to quantify biofilms. Moreover, as the specificity and selectivity of these cationic dyes to polyanions were investigated, they are not always reliable detectors of EPS [9]. The different published studies vary considerably in the protocol, such as the number of washing steps, the conditions of washing (automatic or not, water, phosphate-buffered saline), the duration of crystal violet staining, and the concentration of 0.1 wt% crystal violet solution for 15 min used [10-12].

SI-6. Repetitive SECM line scans over tape-stripped biofilm

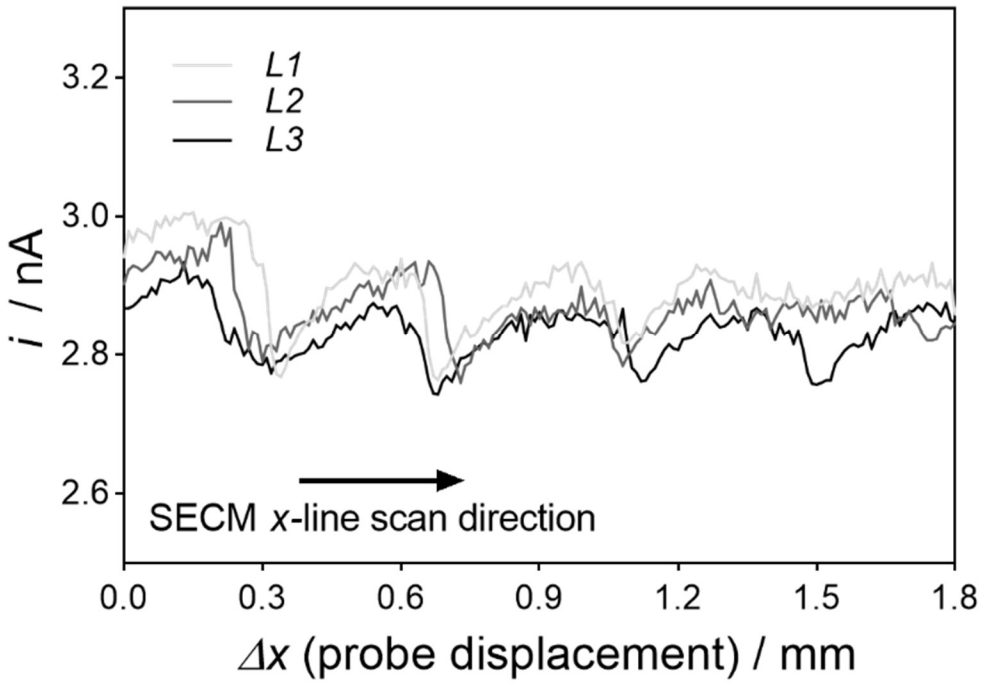

Figure S6. Repeatability of Soft-Probe-SECM line scans over one *E.coli* biofilm surface layer, collected with an adhesive tape. Three line scans *L1* to *L3*. Experimental details: E_T = 0.5 V, probe translation speed = 25 µm/s, step size = 10 µm, 2.5 mM FcMeOH in 100 mM PBS (pH = 7.4).

SI-7. Calibration of SECM currents

Equations for the calibration of the SECM currents in Fig. 4:

$$I^{*}_{\text{solution bulk}} = I_{\text{solution bulk, AC}} - I_{\text{insulator, AC}} \qquad \text{Equation-1}$$

where $I^{*}_{\text{solution bulk}}$ ($I_{\text{sol. bulk}}^{*}$) is calculated by subtracting from the current $I_{\text{solution bulk, AC}}$ ($I_{\text{sol. bulk}}$), measured in the solution bulk at the beginning of an approach curve (AC), the negative feedback current with the soft probe in contact with the insulating surface of the substrate ($I_{\text{insulator, AC}}$). For the bar plots, Eq-2 is used,

$$I_{\text{cal,mean}} = \left(I_{\text{mean, FB-image}} - I_{\text{insulator,AC}}\right) \cdot \left(I^{*}_{\text{solution bulk}}\right)^{-1} \qquad \text{Equation-2}$$

where $I_{\text{mean, FB-image}}$ is the average current of all SECM image points either over the biofilm, adhesive layer, or insulator. The mean SECM current is then normalized by the bulk current $I^{*}_{\text{solution bulk}}$. In this way, the purely negative feedback current over an insulating surface is nearly zero and the calibrated $I_{\text{cal,mean}}$ would be equal to 1 if the FB current over the biofilm would be the same as in the solution bulk.

SI-8. Calibration of the SECM FB currents of *E. coli* biofilms that were collected with adhesive tape for 10 days

Table S8. Details about SECM data from **Fig. 4a** and its calibration to create **Fig. S8**. N = number of data points per SECM image.

Day	$I_{sol.\ bulk}$ / nA	$I_{insulator}$ / nA	$I^{*}_{sol.\ bulk}$ / nA	$I_{mean,FB\text{-}image}$ / nA	$I_{cal,mean}$ / nA
1	3.95	0.02	3.93	(1.73 ± 0.54) (N = 10251)	(0.43 ± 0.13) (N = 10251)
2	3.75	0.02	3.74	(1.49 ± 0.54) (N = 10251)	(0.39 ± 0.14) (N = 10251)
3	3.91	0.08	3.84	(1.29 ± 0.35) (N = 10251)	(0.32 ± 0.07) (N = 10251)
4	3.76	0.02	3.75	(0.72 ± 0.24) (N = 10251)	(0.19 ± 0.06) (N = 10251)
5	3.58	0.01	3.56	(0.64 ± 0.37) (N = 10251)	(0.18 ± 0.10) (N = 10251)
6	4.28	0.02	4.26	(0.90 ± 0.38) (N = 10251)	(0.21 ± 0.09) (N = 10251)
7	4.44	0.05	4.38	(2.43 ± 0.33) (N = 10251)	(0.54 ± 0.06) (N = 10251)
8	4.36	0.03	4.32	(2.48 ± 0.25) (N = 10251)	(0.57 ± 0.05) (N = 10251)
9	4.07	0.13	3.94	(1.53 ± 0.78) (N = 10251)	(0.36 ± 0.17) (N = 10251)
10	3.52	0.09	3.43	(1.36 ± 0.62) (N = 10251)	(0.37 ± 0.18) (N = 10251)

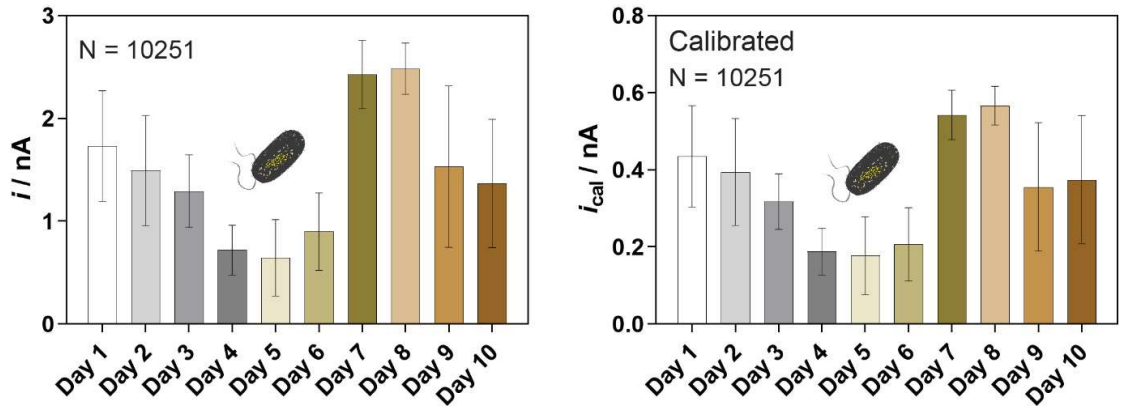

Figure S8. Bar plots show the mean currents ± standard deviation from all data points of ten SECM images of tape-collected *E.coli* biofilm surface layers without (a) and with (b) calibration according to **Table S8**.

SI-9. Soft-Probe-SECM image of bare adhesive tape

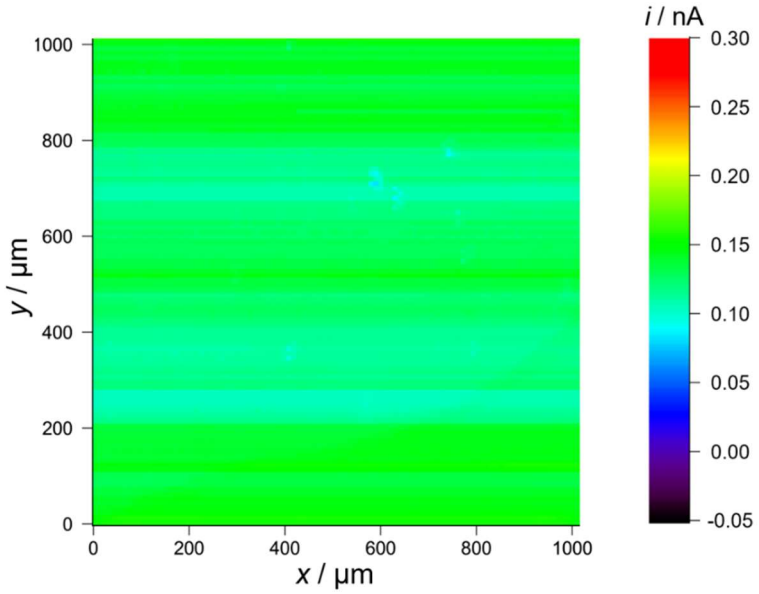

Figure S9. Soft-Probe-SECM FB image of bare adhesive tape. Experimental details: E_T = 0.5 V, probe translation speed = 25 µm/s, step size = 10 µm, 2.5 mM FcMeOH in 100 mM PBS (pH = 7.4).

Table S9. Details about SECM data of the calibration of the SECM FB currents from **Fig. S9**.

$I_{sol.\ bulk}$ / nA	$I_{insulator}$ / nA	$I^*_{sol.\ bulk}$ / nA	$I_{mean,FB\text{-}image}$ / nA	$I_{cal,mean}$ / nA
4.635	0.04	4.59	(0.17 ± 0.05) (N = 10201)	0.11 (N = 10201)

SI-10. Soft-Probe-SECM images of ten *E. coli* biofilms with resistance to ampicillin collected with adhesive tape for 10 days

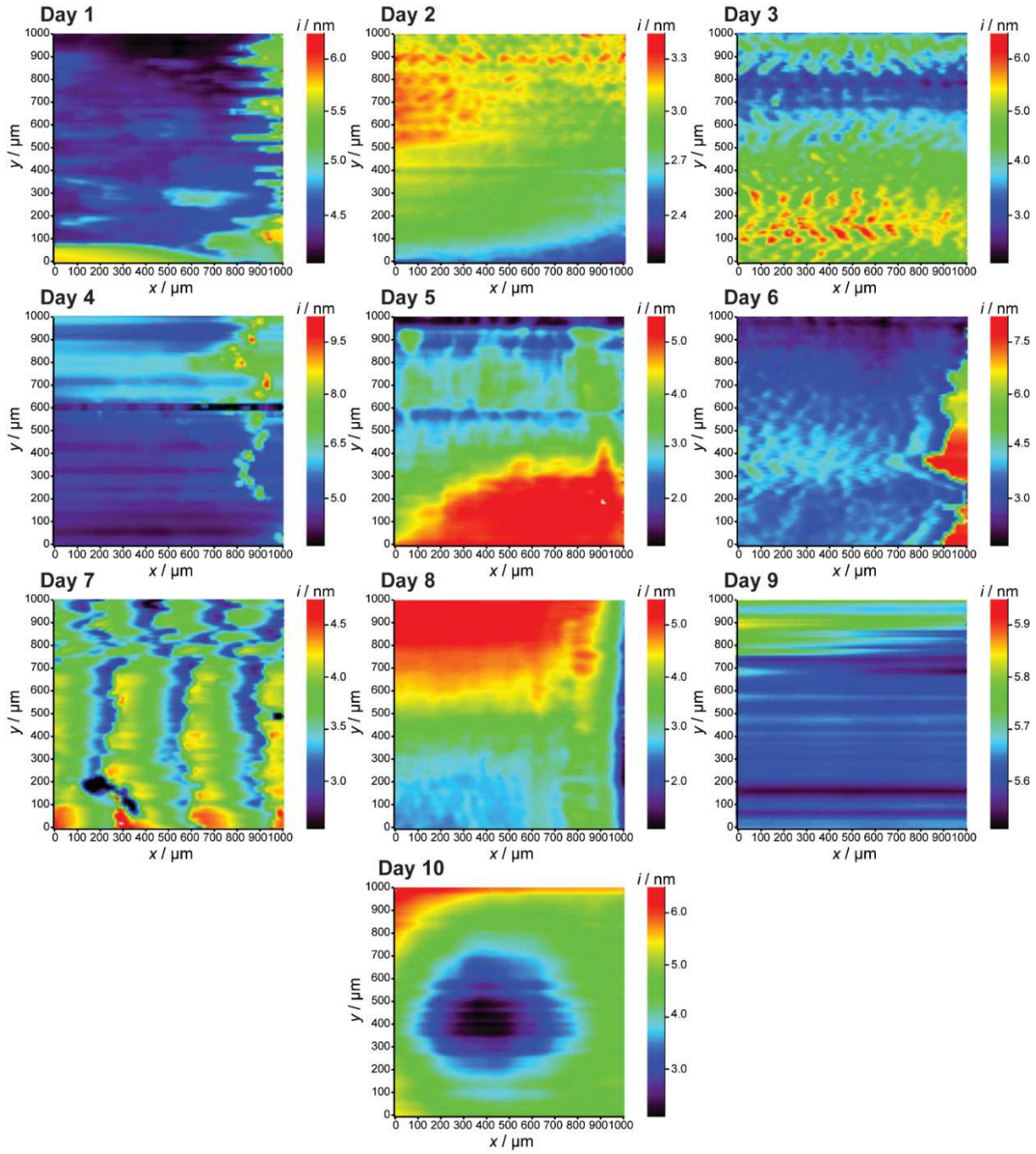

Figure S10-1. Soft-probe-SECM images of resistance *E.coli* biofilm with ampicillin collected with adhesive tape in 10 days. Experimental details: working potential E_T = 0.5 V, probe translation speed = 25 µm/s, step size = 10 µm, 2.5 mM FcMeOH in 100 mM PBS (pH = 7.4).

Table S10. Details about SECM data from **Fig. S10-1** and its calibration to create **Fig. S10-2**. N = number of data points per SECM image.

Day	$I_{sol.\ bulk}$ / nA	$I_{insulator}$ / nA	$I^{*}_{sol.\ bulk}$ / nA	$I_{mean,FB\text{-}image}$ / nA	$I_{cal,mean}$ / nA
1	7.2	0.07	7.14	(4.61 ± 0.41) (N = 10201)	(0.64± 0.05) (N = 10201)
2	8.2	0.07	8.13	(2.83 ± 0.15) (N = 10201)	(0.34 ± 0.010) (N = 10201)
3	6.7	0.05	6.65	(3.80 ± 0.45) (N = 10201)	(0.56± 0.06) (N = 10201)
4	8.1	0.15	7.95	(6.43 ± 0.22) (N = 10201)	(0.79 ± 0.01) (N = 10201)
5	7.3	0.04	7.26	(3.55 ± 0.81) (N = 10201)	(0.48 ± 0.01) (N = 10201)
6	8.3	0.06	8.24	(3.97 ± 0.74) (N = 10201)	(0.47 ± 0.08) (N = 10201)
7	8.1	0.02	7.86	(3.24 ± 0.05) (N = 10201)	0.41 (N = 10201)
8	8.1	0.09	8.01	(3.45 ± 0.83) (N = 10201)	(0.42 ± 0.09) (N = 10201)
9	7.9	0.01	7.89	(5.65 ± 0.08) (N = 10201)	(0.71 ± 0.01) (N = 10201)
10	7.8	0.05	7.75	(4.35 ± 0.68) (N = 10201)	(0.55 ± 0.08) (N = 10201)

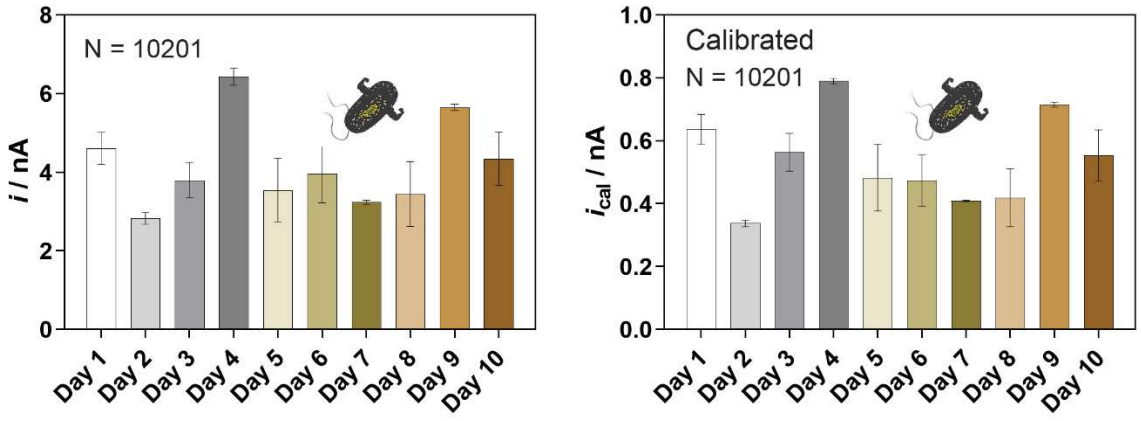

Figure S10-2. Bar plots show mean SECM FB currents ± standard deviation from all data points of ten SECM images of tape-collected *E.coli* biofilm surface layers with ampicillin-resistant *E Coli* cells without (a) and with (b) calibration according to **Table S10**.

References:

[1] J. Maukonen, T. Mattila-Sandholm, G. Wirtanen, Metabolic indicators for assessing bacterial viability in hygiene sampling using cells in suspension and swabbed biofilm, LWT 33 (2000) 225-233, doi:10.1006/fstl.2000.0650.
[2] P.Y. Feipeing, G.A. McFeters, Rapid in situ assessmetn of physiological activities in bacterial biofilms using fluorescent probes, J. Microbiol. Methods 20 (1994) 1-10, doi:10.1016/0167-7012(94)90058-2.
[3] N. Doroshenko, B.S. Tseng, R.P. Howlin, J. Deacon, J.A. Wharton, P.J. Thurner, et al., Extracellular DNA impedes the transport of vancomycin in Staphylococcus epidermidis biofilms preexposed to subinhibitory concentrations of vancomycin, Antimicrob Agents Chemother 58 (2014) 7273-7282, doi: 10.1128/AAC.03132-14.
[4] I.W. Sutherland, The biofilm matrix–an immobilized but dynamic microbial environment, Trends Microbiol 9 (2001) 222-227, doi:10.1016/S0966-842X(01)02012-1.
[5] C. Guilhen, C. Forestier, D. Balestrino, Biofilm dispersal: multiple elaborate strategies for dissemination of bacteria with unique properties, Mol. Microbiol. 105 (2017) 188-210, doi:10.1111/mmi.13698.
[6] F. Cortés-Salazar, D. Momotenko, A. Lesch, G. Wittstock, H.H. Girault, Soft microelectrode linear array for scanning electrochemical microscopy, Anal. Chem. 82 (2010) 10037-10044, doi:10.1021/ac1019304.
[7] G.D. Christensen, W.A. Simpson, J. Younger, L. Baddour, F. Barrett, D. Melton, et al., Adherence of coagulase-negative staphylococci to plastic tissue culture plates: a quantitative model for the adherence of staphylococci to medical devices, J. Clin. Microbiol 22 (1985) 996-1006.
[8] K. Welch, Y. Cai, M. Strømme, A method for quantitative determination of biofilm viability, J. Funct. Biomater. 3 (2012) 418-431, doi:10.3390/jfb3020418.
[9] V. Leriche, P. Sibille, B. Carpentier, Use of an enzyme-linked lectinsorbent assay to monitor the shift in polysaccharide composition in bacterial biofilms, Appl. Environ. Microbiol. 66 (2000) 1851-1856, doi:10.1128/AEM.66.5.1851-1856.2000.
[10] P. Chavant, B. Gaillard-Martinie, R. Talon, M. Hébraud, T. Bernardi, A new device for rapid evaluation of biofilm formation potential by bacteria, J. Microbiol. Methods 68 (2007) 605-612, doi:10.1016/j.mimet.2006.11.010.
[11] P. Naves, G. del Prado, L. Huelves, M. Gracia, V. Ruiz, J. Blanco, et al., Correlation between virulence factors and in vitro biofilm formation by Escherichia coli strains, Microb. Pathog. 45 (2008) 86-91, doi:10.1016/j.micpath.2008.03.003.
[12] A. Reisner, K.A. Krogfelt, B.M. Klein, E.L. Zechner, S. Molin, In vitro biofilm formation of commensal and pathogenic Escherichia coli strains: impact of environmental and genetic factors, J. Bacteriol. 188 (2006) 3572-3581, doi:10.1128/JB.188.10.3572-3581.2006.